Journal of Nuclear Materials 390–391 (2009) 1043–1047

Contents lists available at ScienceDirect

Journal of Nuclear Materials

journal homepage: www.elsevier.com/locate/jnucmat

Physical erosion studies of plain and lithiated graphite

M. Racic, K. Ibano, R. Raju, D.N. Ruzic *

University of Illinois, 104 South Wright Street, Urbana, IL 61801, USA

ARTICLE INFO

PACS:
52.40.–Hf

ABSTRACT

It has been observed that a thin lithium film evaporated on graphite wall tiles in tokamak fusion devices acts to improve plasma conditions. The present focus is to measure the physical erosion rate of various conditions of lithiated graphite under deuterium ion bombardment to help understand this effect. Sputter yields on untreated ATJ-graphite, pure lithium, and lithium-on-ATJ-graphite have been measured for 150, 300, 600 and 1500 nm of evaporated lithium, at an ion energy of 500 eV/ion, 45° incidence, and sample temperatures of 25 and 200 °C by using a QCM to collect the sputtered material. Sputter yields for untreated graphite were measured around 0.06 C-atoms/ion, while yields for pure lithium were around 0.10 Li-atoms/ion. However, combined lithium-on-carbon sputtering yields appeared notably lower than yields for the individual materials. TOF–SIMS analysis was used to estimate relative Li/C levels in collected sputtered material, as well as to look at the concentration versus depth of intercalated lithium in graphite.

1. Introduction

Plasma-facing component (PFC) candidate materials must have material characteristics allowing for high-temperature resilience while limiting particle recycling and core contamination from erosion. Graphite is a good material choice due to its high-temperature resiliency, although it is prone to physical and chemical erosion, which can worsen operating plasma conditions. To reduce deuterium recycling and erosion, lithium has been used as an evaporated coating on plasma facing surfaces [1–3]. In particular, at NSTX (with wall tiles of ATJ-graphite), lithium pellet injection at milligram levels was noted to significantly pump neutral-beam-heated plasmas and results were initially good in reducing deuterium recycling [4]. However, pre-lithium conditions were seen to return in a short time, and the effects were not consistent. It appears that the lithium intercalates into the graphite lattice and acts to getter impurities such as oxygen, forming various oxides and other compounds which interfere with deuterium absorption, requiring a repeated application of lithium to maintain a beneficial effect. It was also observed that recycling and density control in NSTX was not significantly improved when adding much larger quantities of evaporated lithium to the walls [5]. Thicker films were found to be neither more effective nor longer lasting.

Additionally, an observed reduction in the physical sputtering yield of a mixed lithium-on-graphite surface versus the sputtering yields of the pure respective materials is still lacking a full explanation. Previous results of sputtering 150–200 eV helium ions on a Li/C surface describe a reduction of the total carbon sputtering yield to be as low as 1/10 of that of untreated carbon [6]. Part of the work to gain a better understanding of these effects is to experimentally measure and analyze the physical erosion of lithium-on-ATJ-graphite surfaces under deuterium ion bombardment in a controlled environment, where deposited lithium thickness, deuterium ion energies and the surface temperature can be quantitatively varied and studied.

It should be noted here that chemical sputtering occurs as well, though is not focused on in this text. The primary chemical erosion products are acetylene and methane, and given the lithium coating and the high D-ion energies used, the chemical sputtering yield is less than 20% of the physical sputtering yield [7,8]. Furthermore, the quartz-crystal microbalance (QCM) diagnostic used to measure physical sputtering does not collect chemical erosion products in our current experimental setup. It has been modeled to show that at thermal energies, stable gaseous hydrocarbons have a 100% reflection coefficient from the QCM surface [9], and do not interfere with the physical sputtering measurement.

2. Experiment

The current work was performed on the Ion-InterAction Experiment (IIAX). In the past IIAX – in one form or another and called by different names – has been used to measure ion-induced electron emission yields [10], absolute sputtering yields of both solid and liquid metals [11–13], angularly resolved sputtering yields of solid metals [14], and neutral particle reflection.

A Colutron ion source is used to produce a mono-energetic, velocity-filtered, low-energy ion beam to bombard a sample target,

* Corresponding author.
E-mail addresses: mracic2@uiuc.edu (M. Racic), druzic@uiuc.edu (D.N. Ruzic).

0022-3115/$ - see front matter © 2009 Published by Elsevier B.V.
doi:10.1016/j.jnucmat.2009.01.284

with a beam focus diameter of less than 2 mm. The ion beam is focused and calibrated using a Faraday cup, while an E × B filter with variable voltage allows for the selection of solely D_2^+ ions to compose a beam. Ions of D_2^+ are always at 1000 eV, which are considered in all measurements and calculations as 500 eV D-atoms. The deuterium ion flux is stable and consistent at around 10^{13} ions/s (based on current measurement), within the 2 mm beam impact area (or 3×10^{14} ion/cm^2/s) with maximum total fluence of 10^{17}–10^{18} D_2^+ ions within the 2 mm diameter on the target for each trial. Regarding the beam current measurement, since each D_2^+ ion transfers a +1 charge, the current is multiplied by two in all cases to determine the total number of D-atoms (versus D_2^+ ions) impacting the target.

The target consists of a vertically mounted, 1 cm diameter polished ATJ-graphite wafer (obtained from the same supplier as the NSTX wall tiles) at 45° to the ion beam. The graphite sample surface roughness was measured at ±500 nm via profilometry. A water-cooled, dual-unit quartz-crystal microbalance (QCM) is positioned parallel to and a few millimeters from the target to collect and monitor ejected material including sputtered and evaporated components. One crystal, positioned by the target, collects sputtered material while a second shielded crystal acts as a reference. Additionally, a silicon witness plate is positioned at the edge of the QCM deposition-crystal to collect sputtered material for composition analysis (see Fig. 1). The difference in crystal frequencies (each on the order of 6 MHz) between the two units as a function of time, and the ion beam current measurements are the primary data collected and analyzed to determine sputtering yields.

Additional variables are accounted for as constants via calibration experiments, such as the QCM crystal sticking coefficient and oxidation rates of the collected sputtered lithium. The sticking coefficient of sputtered material on the QCM crystal is controlled by first using an Ar^+ beam to sputter a thin amorphous carbon film onto the crystal surface prior to experimental trials. With regard to oxidation effects, the total chamber pressure during the experiments prior to starting the deuterium beam is $\sim 1.0 \times 10^{-5}$ Pa, and $\sim 1.0 \times 10^{-4}$ Pa with the beam on, while the partial pressure of oxygen (O_2 only) with the D-beam off as measured by a residual gas analyzer is $\sim 1.0 \times 10^{-6}$ Pa. At this pressure, molecular lithium oxide forms at a rate of roughly six monolayers per hour, which is the deposition rate of oxygen, following the assumption that all sputtered lithium is oxidized. Additionally, if O_2 is intentionally leaked into the chamber following an experimental run, the mass on the crystal does not indicate a change. Hence, the oxidation of sputtered lithium collected on the crystal is assumed to be complete, forming Li_2O [12].

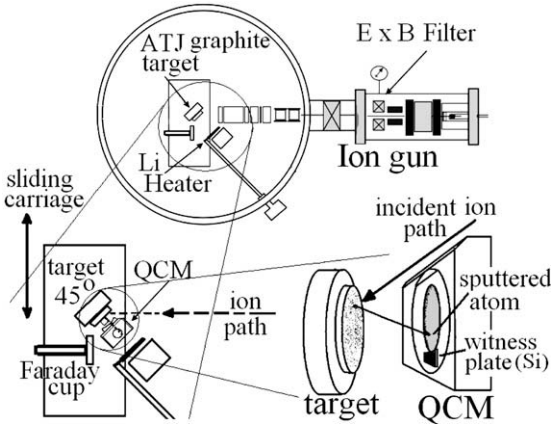

Fig. 1. Schematic of the IIAX experiment. The reference QCM is just below the QCM shown in the figure and in the same housing to share the thermal environment.

The back of the graphite target wafer abuts a high-temperature substrate heater, and the assembly is mounted on a sliding carriage allowing the target to be moved in front of the ion beam or lithium evaporator. Lithium is evaporated *in situ* onto the graphite sample using a simple molybdenum cup with a high-voltage button heater, positioned line of sight of the target, at a distance of 42 mm. The duration of evaporation is controlled by a manual shutter, which is opened only while the lithium is at constant temperature. The lithium deposition was calibrated by profilometry measurements on a masked silicon wafer placed in the target position. Sputtering trials were performed on ATJ-graphite with direct lithium deposition of 150, 300, and 1500 nm, as well as for twice-repeated deposition of 300 nm (for a total of 600 nm) with a one day delay between depositions. It should be noted that the lithium deposited on the graphite sample does not form a distinct layer, but rather rapidly intercalates into the bulk graphite [6]. Therefore, the lithium thickness calibration on silicon should be considered as simply an 'equivalent thickness' with regard to the total amount deposited on the graphite. The lithium deposition rate used in the trials varied from 7 to 12 nm/min.

During the experiments, all lithium is fully deposited on the graphite sample prior to exposure to the ion beam. Due to the relatively slow deposition rate, and the known rapid intercalation rate [15], it can be assumed that the lithium is nearly fully intercalated by the time sputtering measurements begin. Sputtering trials typically can last anywhere from 3 to 30 h, in large part to obtain enough data to outweigh statistical uncertainties due to the very small sputtering yields being measured. Hence, it is assumed that all sputtering measurements are taken from a steady state system.

3. Calculating sputtering yields

The calculation of the sputtering yield is performed by converting the rate of frequency change of the QCM crystal into an equivalent mass deposition rate in atoms/s. The sticking coefficient of sputtered material is near 100%. This deposition rate is then divided by the ion beam dose in ions/s, to indicate a sputter yield of atoms/ion. Furthermore, this yield must be divided by the fraction of sputtered material collected on the crystal to obtain the absolute sputter yield. This fraction is calculated by integrating the distribution of ejected material (cosine distribution) over the solid angle subtended by the QCM crystal, assuming the beam impact position as a point source.

To obtain a better overall system calibration for the calculation of sputter yields for the mixed Li/C samples, baseline measurements and calibrations were performed at room temperature of 22 °C with a 1000 eV D_2^+ beam (equal to 500 eV/D-ion) on pure ATJ-graphite and on pure lithium-on-stainless-steel. For ATJ-graphite, literature gives yields from 500 eV D^+ at normal incidence to be between 0.025 to 0.04 C-atoms/ion [16], with a nearly factor of two adjustment made for the 45° incidence used here [17], predicting yields between 0.04 to 0.07 C-atoms/ion. For pure Li, published yields are ~0.10 Li-atoms/ion [12] at 45°. The measured results of these baseline trials at room temperature were measured to be 0.10 ± 0.04 Li-atoms/ion and 0.06 ± 0.03 C-atoms/ion, respectively. Also noted is that the mass of lithium oxide (Li_2O) at 29.88 g/mol is used in place of the mass of pure lithium when converting the QCM frequency to a mass, due to the complete oxidation assumption stated above.

For the mixed lithium-on-graphite trials, it is necessary to estimate the ratio of sputtered atoms to calculate the respective yield contributions. The silicon witness plate by the QCM crystal is removed and is measured *ex situ* by TOF–SIMS using an oxygen beam. Even though atmospheric contamination will occur, the ratio of the elements on the silicon sample remains invariant to that

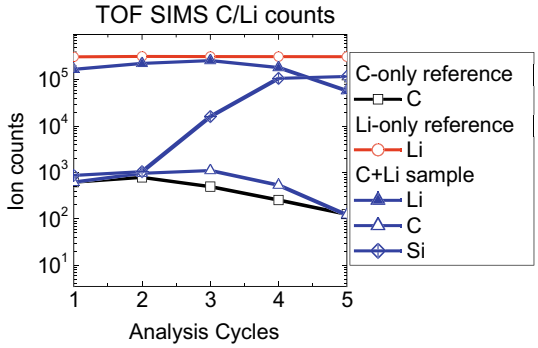

Fig. 2. TOF–SIMS results showing counts of Li and C of the sputtered mixed sample collected on the witness plate, versus the pure material reference counts, for 1500 nm Li/C at 25 °C, for about 10 nm in depth on the witness plate. There are more data points on each curve than shown by the legend markers. The high-count stabilization of the Si count marks the bottom of the collected sputtered material on the witness plate.

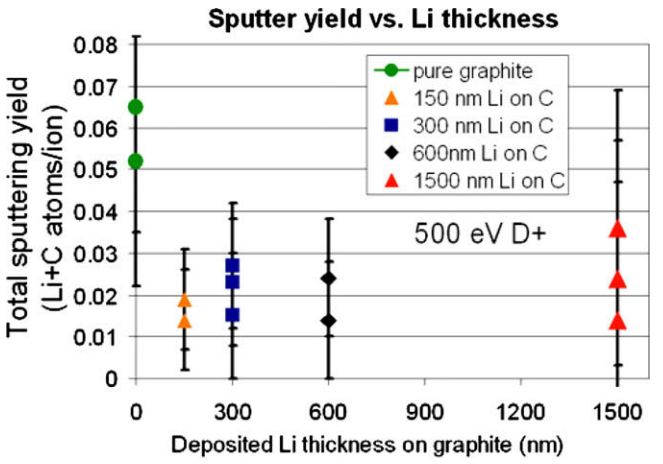

Fig. 3. Plot of data points for Li + C sputtering yields versus thickness at 45 degree incidence. Pure Li was also measured at 0.10 ± 0.021 Li-atoms/ion.

of *in situ* samples, provided one reaches the appropriate total ion fluence on the Li/C wafer of near 10^{16} cm^{-2} [18] which provides a few monolayers of coverage at minimum. At this point, the deposited sputtered particle layer on the witness plate is sufficiently thick to allow stoichiometric erosion by the SIMS beam below the thin passivated surface layer. Two silicon reference plates sputtered with pure lithium (which fully oxidizes into Li_2O as well) and pure carbon, respectively, were also measured to obtain 'pure' material reference counts at the same beam parameters as the Li + C silicon witness plates. The percent decrease of the lithium and carbon counts, respectively, on the mixed sample compared to the counts for pure reference samples can point to the composition ratio. The sum percent of the residual counts of each material (for the mixed sample) should ideally add to 100%. However, because of the very low ionization rate of carbon, the carbon counts varied widely and were not deemed reliable. It is expected that there will be matrix effects, but the aim is only to measure relative concentrations. The lithium achieved consistently high counts 1000 times stronger than those for carbon, and very consistently showed a 10% to 15% decrease in counts for the Li/C mixed samples (see Fig. 2). Therefore, the lithium fraction is taken to be 85% to 90% of the total mixed-sample sputtered material in calculating yields, and the carbon fraction is assumed as the remainder. However, given that there are certainly unknown matrix effects in the TOF–SIMS measurements, this percent composition cannot be taken as a definite value, and this matrix effect uncertainty contributes substantially to the error in determining the sputtering yield.

This ratio is also in good agreement with prior related work using helium ion sputtering [6]. It should be noted that some of the Li count decrease in TOF–SIMS could also be attributed to the presence of carbon causing a reduction in the typical ~60% pure-Li sputtering ionization fraction [11]. However, the Li/C sputtering products would still then be shown to contain primarily lithium, as such an ionization reduction would imply the true Li fraction would then be higher than 85%. This further implies a large amount of diffusion of Li to the surface at a fast rate [15]. More importantly, though, the fact that TOF–SIMS identifies substantial lithium levels in the mixed sputtered material does not disprove the concept that lithium is continually supplied to and sputtered from a Li/C surface.

4. Results and discussion

4.1. Lithium-on-graphite sputtering

In general, the sputtering yields for 150, 300, and 600 nm of Li-on-C can be thought to be reduced compared to the sputtering yield of carbon alone. Looking solely at the calculated yield data points, the reduction appears quite consistent at a factor of about 1/3 of the measured pure C yield. However, when taking the experimental error into account, the claim of yield reduction cannot be made with complete certainty, despite much evidence pointing to it. Additionally, the potential formation of other volatile surface compounds was not taken into account here, though may contribute to the total mass collected.

The yield of 500 eV D-atoms (from the beam of 1000 eV D_2^+) on 150 nm Li/C is at an average of 0.016 ± 0.012 [atoms/ion]. The yield from 300 nm Li/C is at an average of 0.022 ± 0.016 [atoms/ion]. The yield for 600 nm Li/C is at an average of 0.019 ± 0.014 [atoms/ion]. The scatter between calculated data points for these three thicknesses is within a range of 0.01 [atoms/ion]. While there appears to be a consistent yield reduction, it must be noted that the error bars overlap between the pure C and these Li/C trials. In the case of 1500 nm Li/C, the results are somewhat more unclear. The average of the calculated yield values is 0.020 ± 0.03 [atoms/ion], which is in the same region as that of the other trials. However, tests at this thickness had a significantly higher uncertainty, and as a result, the error bars overlap significantly with the pure C trial (see Fig. 3).

It is not entirely unexpected that the yield at 1500 nm would be higher than that of lower deposited thicknesses. Part of the reason for choosing this thickness was to deposit a sufficient Li thickness to overcome and entirely cover the entire range of surface roughness of the ATJ sample. With an ever thicker deposition, it was thought logically that the yield should eventually revert to that of pure Li alone. However, in contrast to this thought are the results [15] where even a full 3 μm of Li were deposited and observed to fully intercalate rapidly. This would imply that the surface condition at 1500 nm of Li should still be roughly the same as that of the lower thicknesses. In the end, it remains unclear which of these two lines of thought best describes the surface conditions with 1500 nm of Li. However, all found literature only supports the latter conclusion, and it is most likely that the sputtering yield remains suppressed under 1500 nm Li deposition, and that the Li in this case fully intercalates as well.

Additionally, the Li was never all sputtered during the trials. This would imply a similar surface layer structure for all thicknesses tested. These suppression results are in good alignment with previous work, which tested Li/C yield suppression using 200 eV He on 0–300 nm Li-on-graphite [6]. The authors reported that marked sputtering suppression occurs with as little as 25 nm of Li, and indicated that the suppression rate stabilizes above 300 nm Li.

The exact reasons for the overall yield suppression are still unclear, although appear to be related to the formation of lithium oxides. A Li/graphite surface was found by *in situ* XPS to contain predominantly lithium peroxide (Li_2O_2) [19]. A higher surface binding energy of Li in this compound compared to that of pure lithium could explain the reduced Li yield. The reduced carbon yield could be explained by a large presence of lithium in some form at the top monolayers, preventing carbon sputtering [6]. However, the sputtered lithium fraction remaining consistently high requires a mechanism of resupplying Li to the surface, likely through intercalation [6]. A (unsubstantiated) possibility is that a consistently small amount of free lithium is continually replenished via intercalation to the top monolayer around the lithium peroxide molecules, and that this free lithium is sputtered or evaporated. Key questions to identify are how much free lithium might diffuse to the top monolayer and remain unoxidized before being sputtered, whether sufficient free lithium would be able to diffuse around the indicated Li_2O_2 molecules (which are obviously too large to intercalate into the bulk), and whether it is a small fraction of such free lithium that is being continually sputtered and replenished, rather than lithium atoms broken free from the peroxide bond. The rate of replenishment could then be the limiting factor in the reduced Li sputtering yield. Given that the oxidation rate at our oxygen partial pressures indicates surface oxidation at a faster rate than the sputtering rate, it is quite likely that our 500 eV beam is sputtering and disassociating Li_2O_2 from the surface. In much stronger vacuum conditions, however, there may then be free Li intercalating to the surface that is sputtered before being oxidized.

To examine the concept that lithium is being supplied from the bulk, TOF–SIMS was also performed on a previously sputtered 1500 nm Li/graphite wafer in three surface regions: on a sputtered spot (sputtered for 20 h, with Ar for this test, which should produce a hole on the order of 1 to 2 microns), on an untouched Li-deposited area, and a shielded region for carbon count reference. The goal was to obtain a comparative depth profile of lithium, to see if the lithium concentration versus depth was reduced below the sputtered spot compared to the undisturbed region. Data was obtained using an equivalent TOF–SIMS beam and measurement duration for each spot, and taken until the carbon count became steady at 100% of the clean-reference-spot carbon count, with the undisturbed sample as a basis for the test duration. The results show that the undisturbed-region Li counts at the deepest point are 81% of the surface counts, versus 61% at the sputtered spot. The near-surface Li counts are equivalent at both spots, and the surface carbon counts for both spots are identical, and are 30% of the counts at the deepest point (see Fig. 4). This suggests that lithium was intercalating up from the bulk graphite in the region below the sputtered spot, and was replenishing the surface during the original sputtering trial. It should be noted that the same mechanism acting to supply Li to the surface during deuterium erosion likely occurs in this TOF–SIMS test as well. Therefore, the concentration depth profile is likely not an accurate measure of the original Li concentration versus depth, but likely provides a combination of the original Li depth concentration and the Li supply toward the surface from the bulk during sputtering.

4.2. Temperature dependent sputtering

Sputter yields were also measured for a 200 °C heated target for 1500 nm of Li-on-graphite, with the same deuterium flux of 10^{13} ions/s over the 2 mm diameter sputtered spot. This temperature was chosen because an evaporative Li flux would potentially exist, but not be so strong as to outweigh the sputtered particle yield. The average calculated yield based on the QCM signal provided a result about 25% higher than the average yield value from the room

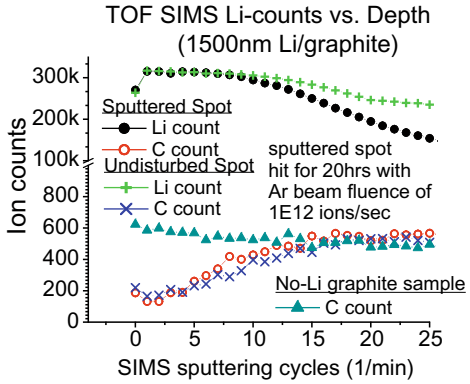

Fig. 4. TOF–SIMS results showing relative Li concentration versus depth, comparing a sputtered and undisturbed region for a 1500 nm Li-on-graphite wafer. The depth at the right end of the figure corresponds to approximately 2 ± 0.5 microns, with uncertainty due to graphite surface roughness.

temperature test. However, when taking into account the uncertainty in the results, no conclusion of temperature enhanced yield can be made. This includes the uncertainty of how to take into account the known evaporative flux of Li at this temperature. The evaporative flux of lithium under high temperature is not clear when in combination as a Li/C mixed surface, and would be dependent on surface oxidation rates, among other variables. Lithium peroxide existing on the surface, as suggested by XPS measurements [19], would not evaporate at this temperature, which would imply a minimal evaporative flux of Li and possibly a larger true sputtering yield at 200 °C.

In contrast, the evaporative Li component from the target surface (if pure lithium) would be estimated to add approximately 20% to the sputtered material collected on the QCM. Subtracting this component would provide nearly the same mixed sputtering yield as a 25 °C target. Previous work has indicated that pure-Li sputtering yields are not heat-enhanced at temperatures below 280 °C [20]. One may assume that this behavior holds true for Li/C surfaces as well, and that the gain in yield is a result of Li evaporation. Furthermore, TOF–SIMS found 92% sputtered lithium, suggesting the existence of free, evaporating lithium in the top monolayer, despite the report of the large Li_2O_2 XPS peak. The higher lithium percentage could also arise from a heat induced easing of the diffusion of Li to the surface.

As a final consideration, although free lithium may exist in the top monolayers, it appears to still be somehow inhibited in pumping deuterium, such as in NSTX, once all deposited Li has fully intercalated. Verifying the true surface composition has important implications for understanding the surface evolution during reactor test shots, and would help better explain the reason for reduced overall Li/C sputtering yields.

5. Conclusion

Lithium in equivalent thicknesses between 150 to 1500 nm were evaporated onto ATJ-graphite, and sputtered by 500 eV deuterium ions. Total physical Li + C sputtering yields for thicknesses between 150 and 600 nm of Li/C were recognized as being suppressed compared to yields of pure graphite and lithium, which agrees with other published results. However, noting the experimental error, this observation cannot be proven outright. For 1500 nm of Li/C, sputtering yield suppression is also suggested, but cannot be conclusively determined. Within the parameters of this experiment, given the oxidation rate greater than the sputtering rate, the observed sputtering reduction is most likely from lithium oxides (with high binding energy) covering the carbon due to

lithium continually diffusing to the top monolayers. In a higher temperature case, an enhanced diffusion rate of lithium to the surface may cause the rate of lithium supply to the surface to exceed the oxidation rate, enhancing evaporation and preferential sputtering of free lithium, although not increasing the physical sputtering yield of carbon. In all trials, chemical erosion was determined not to play a role in the measurements. Lithium deposited on graphite is known to rapidly and fully intercalate into the graphite bulk, although the sputtered Li + C material composition was suggested to still contain primarily lithium. The concept that lithium is continually being replenished from the bulk was initially verified with TOF–SIMS. However, the question remains whether the sputtered lithium source and associated yield reduction is from limited free lithium intercalating to the top monolayers or from lithium oxides present at the surface. In any case, lithium treated graphite does appear to provide substantial benefits over plain graphite in the operation of fusion devices, and merits continued use and investigation.

Acknowledgments

This work is supported by DOE/ALPS Grant No. DE-FG02-99ER54515, and this material is based upon work supported under the National Science Foundation Graduate Research Fellowship. Also we would like to thank Tim Spila for his help with TOF–SIMS measurements carried out in the Center for Microanalysis of Materials, University of Illinois, which is partially supported by the US DOE Grant Nos. DE-FG02-07ER46453 and DE-FG02-07ER46471. In addition, we would like to thank J.P. Allain for many helpful insights and discussions.

References

[1] D.K. Mansfield et al., Phys. Plasmas 3 (1996).
[2] R. Majeski et al., Phys. Rev. Lett. 97 (2006).
[3] R. Kaita et al., Phys. Plasmas 14 (2007).
[4] H.W. Kugel, R. Majeski, R. Kaita, in: DOE PFC e-Meeting, September 2006.
[5] H.W. Kugel et al., J. Nucl. Mater. 363–365 (2007) 791.
[6] S. Kato, M. Watanabe, H. Toyoda, H. Sugai, J. Nucl. Mater. 266–269 (1999) 406.
[7] H. Yagi et al., J. Nucl. Mater. 313–316 (2003) 284.
[8] L.I. Vergara et al., J. Nucl. Mater. 347 (2005) 118.
[9] D.A. Alman, D.N. Ruzic, Physica Scripta T111 (2004) 145.
[10] P.C. Smith, B. Hu, D.N. Ruzic, J. Vac, *Sci. Technol. A* 12 (1994) 2692.
[11] J.P. Allain, D.N. Ruzic, M.R. Hendricks, J. Nucl. Mater. 290–293 (2001) 33.
[12] J.P. Allain, D.N. Ruzic, Nucl. Fusion 42 (2002) 202.
[13] J.P. Allain, M.D. Coventry, D.N. Ruzic, J. *Nucl. Mater.* 313–316 (2003) 641.
[14] P.C. Smith, D.N. Ruzic, Nucl. Fusion 38 (1998) 673.
[15] N. Itou, H. Toyoda, K. Morita, H. Sugai, J. Nucl. Mater. 281–285 (2001) 281.
[16] R. Behrisch, W. Eckstein (Eds.), Sputtering by Particle Bombardment, 2007, p. 45.
[17] T. Ono et al., J. Nuc. Mater. 363–365 (2007) 1266.
[18] J.P. Allain, UIUC, May 2008, private communication.
[19] D.P. Stotler et al., Phys. Plasmas 15 (2008) 058303 (Summary of Mini-Conference).
[20] J.P. Allain et al., J. Nucl. Mater. 313–316 (2003) 641